Prepared for submission to JCAP

On the extension of the sensitive area of an extensive air shower surface array

H. Hedayati Kh.

Department of Physics, K.N Toosi University of Technology, P.O. Box 15875-4416, Tehran, Iran

E-mail: hedayati@kntu.ac.ir

Abstract. A large distance between true and reconstructed core locations of an extensive air shower (EAS) may results in great systematic mis-estimation of EAS parameters. The reconstruction of those EASs whose core locations are outside the boundary of a surface array (outside EAS (OEAS)) results in a large distance of the reconstructed core location from the true one, especially when the true core is far outside the array. Although it may not be mentioned, the identification of OEASs is a necessary and important step in the reconstruction procedure of an EAS. In this paper, an existing technique is optimized for the identification of OEASs. The simultaneous use of this technique and a recently developed approach for reconstructing the core location of an EAS can significantly increase the sensitive area of a surface array.

Contents

1 Introduction

In a surface array during an EAS event, a particularly minimum number of array detectors should be usually triggered to record the event (threshold condition). Sometimes, an EAS with the true core outside the array boundary can satisfy the threshold condition. Reconstructed core location of these EASs not only is inside the array, but may also have considerable distance from array boundary, especially for those EASs with the true core far outside the array.

This problem may sometimes be even worse. For some OEASs, a few number of array detectors may exists that, in spite of the large distance from the true core location, detect a significant number of particles. Often, the reason of this event is a single particle of the EAS that moves behind the EAS front and, as a result of Landau fluctuation and or a cascade in detector material, generates a large pulse height which is mistaken for a high particle density location. Corrupted data of these detectors in addition to destructive effect on the reconstruction of the EAS direction may cause difficulty on the rejection of such EASs as OEASs even with sophisticated core location reconstructing algorithms.

In short, identification of OEASs is very important, since if the distance of the reconstructed core location from the true core of an EAS is large, in addition to a systematic tilt in reconstructed arrival direction of the shower, its other reconstructed parameters such as shower size, age parameter, etc. will have significant systematic errors.

There are various methods to identify OEASs in a surface array. A sophisticated method for the identification of OEASs is using complementary data other than those of the surface array detectors alone (e.g. data of Cherenkov light detectors [1]). The disadvantages of these techniques are that they raise the cost of the array construction and, in some cases such as air Cherenkov detectors, restrict the duty factor of the array considerably (e.g. to a dark clear moonless night).

If one merely relies on data of a surface array detector, the most common method is the border cut (e.g. KASCADE-Grande [2]): Based on this approach, the reconstructed core and the first guess core position have to be deep inside the boundary of the array. Furthermore, it is required that the station containing the largest signal is not on the border of the array. Although the perimeter area of an array is a narrow region, it usually has a considerable contribution to the total area of the array. So, this technique reduces the overall efficiency of the array (defined as the probability by which an EAS whose core is inside the array boundary will remain in the final event sample). Also, it can reduce the energy extent of detected EASs by the array, because the most energetic EASs which can be detected by an array are those EASs with the true core near the boundary [3].

An interesting technique for the rejection of OEASs is to find the weighted mean of distances of the registered particles from the reconstructed shower core [4], as named by authors as r_p:

$$r_p = \frac{\sum_{i=1}^{N} \alpha_i n_i r_i}{\sum_{i=1}^{N} \alpha_i n_i} \tag{1.1}$$

The summation includes all triggered detectors in the array. The parameter r_i represents the distance of the ith detector from the center of gravity (COG) of the responding detectors, n_i the particle density measured by the ith detector, and α_i a weight which takes into account the inhomogeneous detector spacing in an asymmetrical surface array. The weights are inversely proportional to the density of detectors around the ith detector. According to the authors, exceptionally large distances between the true and reconstructed shower cores results in exceptionally large r_p values, so OEASs can be identified by their r_p values (actually we will see below that when the true core is outside the array, contrary to authors' view, using distances from the true core location as r_is results in the greatest r_ps). So, when we use a common method for the reconstructing core location, this technique can only identify far OEASs and still need a relatively large border cut.

Sophisticated techniques such as neural networks [5] cannot drastically improve the above methods and the true core location must be inside array and have significant distance from the array border in order to be reconstructed reliably.

In this paper, r_p parameter will be optimized for the identification of OEASs. This identification technique relies only on the surface array data and can increase sensitive area of an array. For the real EASs, we do not have the exact core location, so they are not suitable for comparing the results of different methods for the identification of OEASs. Therefore, in order to prove the functionality of this technique, simulated EASs whose specifications are introduced in the next section are used.

2 Air Shower Simulations

In order to confirm the performance of OEAS's identification parameter, more than 400,000 CORSIKA version 7.4 [6] simulated EASs whose specifications are summarized in Table 1 were generated.

A hypothetical surface array, similar to that of [3] (a square array with 21×21 detectors, the network constant of 10m over the total area of $200 \times 200\text{m}^2$) is applied (Fig. 1). A threshold condition of triggering at least 12% (53 detectors) of array detectors is exerted. For finding the arrival direction, plane front approximation is used.

3 Outside showers identification parameters (OSIP)

Any parameter which can be used as an OSIP should have a different behavior for an OEAS compared with an internal EAS. For example, the mean value function of OSIP should change

Specification	Value
geographical longitude	51 E
geographical latitude	35 N
altitude	1200 m
earth magnetic field (B_x)	28.1 μT
earth magnetic field (B_z)	38.4 μT
low energy hadronic model	Fluka 2011.2b [7]
high energy hadronic model	QGSJETII-04 [8]

Table 1: EASs' specifications. Other specifications are CORSIKA default values. The primary particle of 90% of the showers are protons and the remaining primary particles are alphas.

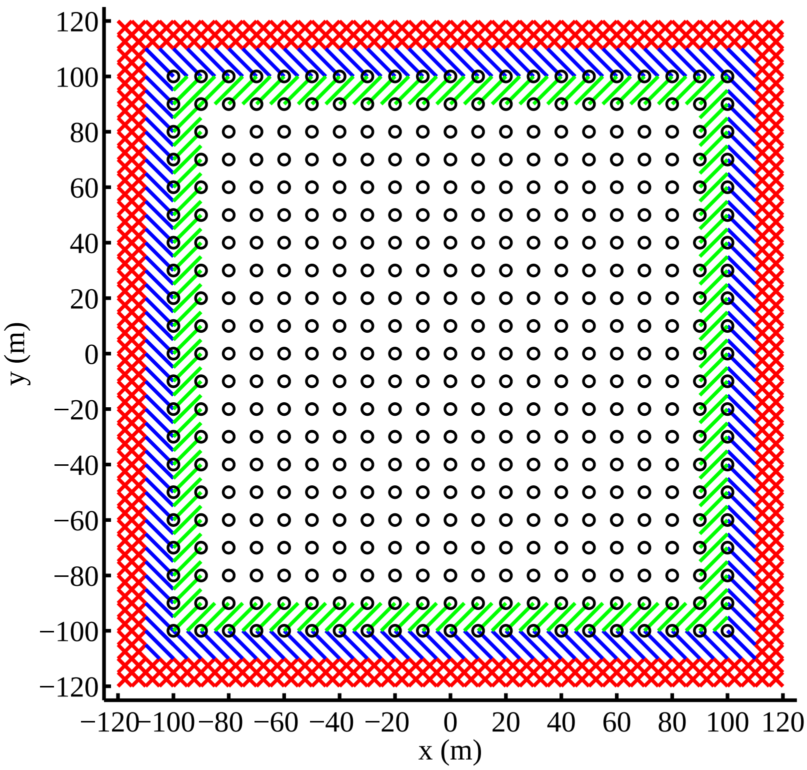

Figure 1: Layout of the assumed array. The positions of detectors in the array are shown by empty black circles (not to scale). The last internal ring of the array is hatched by green lines. Also, the first and second external rings are shown in this figure.

its trend on a smooth boundary line of an array. But, we should have in our mind that the change of behavior condition (e.g. change of mean value curve trend) of a parameter on the border of the array is a necessary, not an enough, condition. For example, a parameter which has different mean values in and out of an array may has very wide overlapping distributions inside and outside the array and cannot be used as an OSIP.
At first, we begin our consideration with r_p using COG as the core location (as the inventors of r_p have proposed). Our hypothetical array is symmetrical and the density of detectors

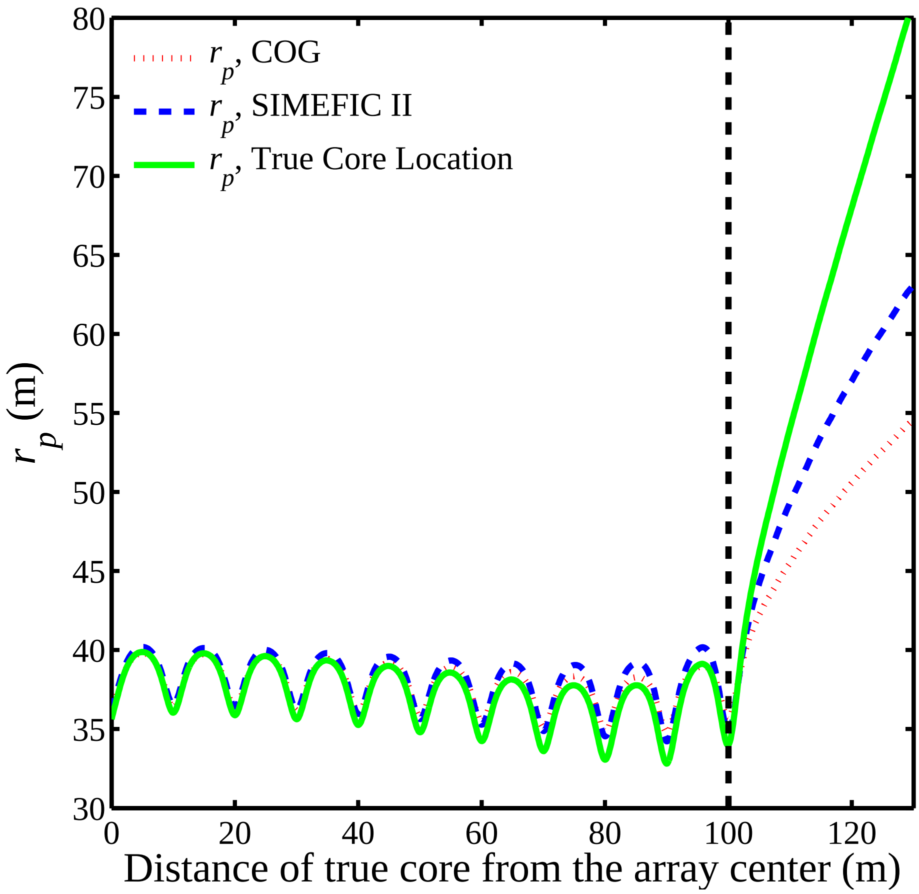

Figure 2: Dotted red line belongs to the average of r_p on horizontal symmetry line of the array for the aforementioned EASs which satisfies threshold condition. The dashed blue line belongs to the results of r_p using SIMEFIC II for the reconstruction of core location. The solid green line belongs to the results of r_p in its ideal form. Border location (side of the array) is depicted by a vertical dashed black line.

around every detector of the array is the same in all parts of the array, so we should substitute $\alpha_i = 1$ for all is in Eq. 1.1.

In order to compare the behavior of the mean value function of r_p inside and outside the array, the true core location of each EAS is assumed to be on the line $(i, 0)$ (i increases from 0 (array center, on (0,0)) to 130m outside the border line of the array by steps of 1m). In each step, the r_p is averaged for those EASs that satisfy the threshold condition.

As can be seen in Fig. 2, average of r_p (dotted red line) on the border of the array changes its slope and beyond the array border, its mean value quickly increases. So, we expect that a shower with larger r_p is more probable to be an OEAS compared with a shower with smaller r_p.

In order to optimize the r_p parameter to be used as an OSIP, we reconstruct the core location of the shower by a more precise method than COG of responding detectors. SIMEFIC II method [9] has far better results than COG for reconstructing the core location of an EAS. For reconstructing the core location, SIMEFIC II (M=N/4, Cx=2, Cy=2) which has relatively good precision near the border of the array is used. As can be seen in this figure, when we

reconstruct the core location by the SIMEFIC II method (dashed blue line), the slope change of the mean value is even more severe.
In Fig. 2, r_p is also shown in its ideal form (solid green line). In this situation, r_is are distances to the true core location of an EAS (provided by CORSIKA). It shows the ultimate limit for using r_p as an OSIP. As can be seen, SIMEFIC II makes r_p closer to its ultimate behavior in the outside region. Another interesting fact is that, when the core location is outside the array, if someone can reconstruct a core location near the true core location, OEASs can be better identified.

4 Distribution Functions

As said in the previous section, the trend change is only a necessary, not an enough, condition. Another necessary condition for a good OSIP is that its probability distribution should be narrow enough which can efficiently discriminate between a deep OEAS and an internal EAS with the true core location near the boundaries (especially the last internal ring).
In order to evaluate the qualification of an OSIP to fulfill this necessary condition in our assumed array, at least an OSIP should discriminate between an EAS with the true core location in the last internal ring of the array (green hatched area in Fig. 1) and the second external ring (red crosshatched in Fig. 1). So, we distribute EASs' true core location uniformly in each of the 3 regions shown in Fig. 1 (as mentioned in Sec. 2) and, then, evaluate the cumulative distribution functions (CDF) of OSIPs for each area (the true core locations of each EAS are uniformly distributed on each region for 10 times and, whenever an event satisfied the threshold condition, it is applied).
Figure 3a shows the results of CDF of r_p using COG as the reconstructed core location, Fig. 3b shows the results of using SIMEFIC II reconstructed core location for the CDFs of r_p, and Fig. 3c shows the results of r_ps CDFs in its ideal form (r_is are distances from the true core location). It is clear that r_p in its ideal form at most can distinguish the last internal ring's EASs from the second external ring's OEASs nearly completely (when all the second external ring's OEASs are rejected, we can be sure that all OEASs from regions beyond it will be rejected as well (see Fig. 2)). But, even when we reject the second external ring completely, we have a large contribution from the first external ring. Also, it can be seen that SIMEFIC II can make r_p a significantly better OSIP than using r_p with COG, because it can hold more events from the last internal ring and, at the same time, reject all the events from the second external ring.
Table 2 shows some interesting values extracted from CDF of the above OSIPs. In this table, we choose the values for the OSIPs whose contamination of OEAS from the second external ring will be less than or approximately equal to 0.5%. As can be seen, when we optimize r_p, the contribution of the last internal ring will be increased by about 9% compared with the non-optimized r_p. At the same time, contamination from the first external ring will increase again by about 9%.

5 Core location precision

Because the area of the first external ring is more than that of the last internal ring, it may seem that those events which will remain from the first external ring in the survived EASs can destroy precision of all the others (especially because of their great error in the reconstruction of core locations). But, because of the correction term in SIMEFIC II method, we

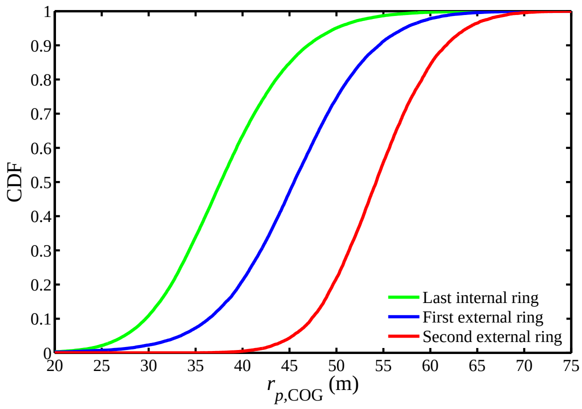

(a) COG is used as the core location.

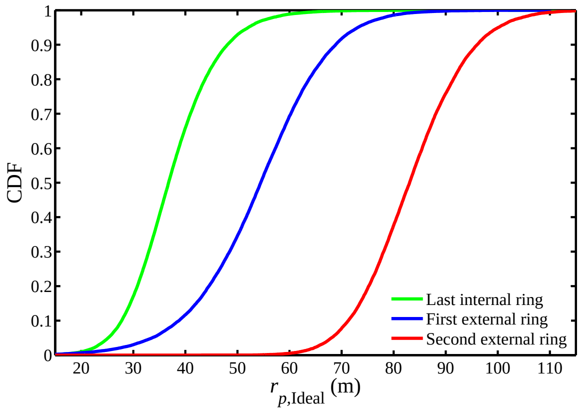

(b) r_p in its ideal form (true core location provided by CORSIKA is used).

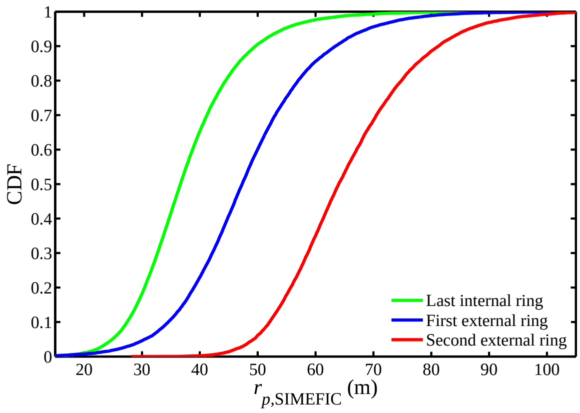

(c) SIMEFIC II method is used for finding the core location.

Figure 3: CDF of r_p in 3 regions of Fig. 1.

can find the core locations of those events from the first external ring with relatively good precision.

In order to estimate the results of the foregoing technique for the precision of reconstructing the core location, the true core location of the simulated EASs is evenly distributed in all three mentioned regions and, then, the error of core location reconstruction is estimated. The

$r_p < r_{p,\max}$	last internal ring	first external ring	second external ring
$r_{p,\mathrm{COG}} < 40$ m	64%	21%	$\lesssim 0.5\%$
$r_{p,\mathrm{SIMEFIC\ II}} < 42.2$ m	73%	30%	$\lesssim 0.5\%$
$r_{p,\mathrm{ideal}} < 59.9$ m	99%	69%	$\lesssim 0.5\%$

Table 2: Some remarkable values extracted from CDF curves in Fig. 3. Column 1 shows the maximum values for each OSIP in order to have less than 0.5% event contamination from the second external ring. Columns 2, 3, and 4 show the percent of accepted events by OSIP from each region.

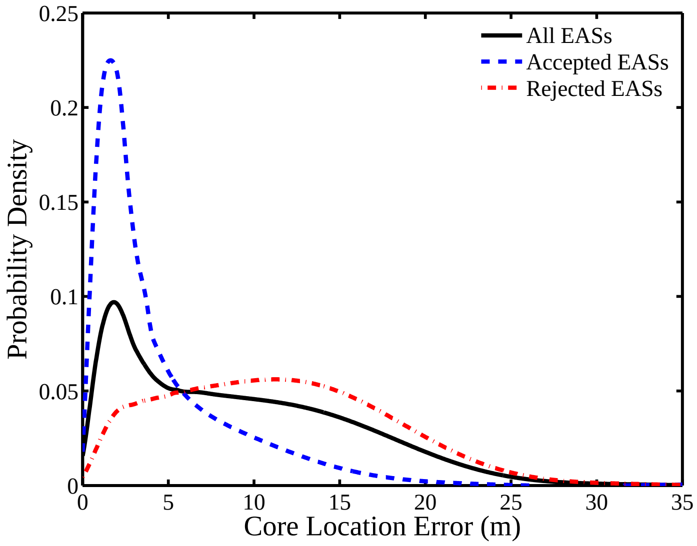

Figure 4: Distribution of the distance between the reconstructed core location and the true axis.

results are shown in Fig. 4. In this figure, distribution of distances of the reconstructed core location by SIMEFIC II ($M = N/4, C_x = 2, C_y = 2$) from the true axis of EAS (which is a measure of the reconstructed core location error [9]) for those EASs which satisfy the trigger condition is shown. As can be seen, when we use the rejection condition ($r_p < 42.2$m using SIMEFIC II for finding r_is), the error occurring in core location reconstruction procedure is far better (with the mean value of 4.4 m). Also, you can see in this figure that the rejected EASs have far worse precision than the selected EASs (the mean value of error is 11.4 m). Actually, with this rejection condition, 32% of those EASs which are accepted in the trigger condition will remain. The area of the three shown regions altogether is $220\text{m} \times 220\text{m} - 190\text{m} \times 190\text{m} = 12300\text{m}^2$. Therefore, the sensitive area of the array is increased by about $0.32 \times 12300\text{m}^2 = 3936\text{m}^2$. If we compare this area with the area of the array with the border cut of 10 m, the array's area without the last internal ring (that would be $190\text{m} \times 190\text{m} = 36100\text{m}^2$, an optimistic border cut), the sensitive area of the array will be increased by about 10%, which is more than the area of the last internal ring ($200\text{m} \times 200\text{m} - 190\text{m} \times 190\text{m} = 3900\text{m}^2$). Without this procedure, such an increase in sensitive area needs at least adding a new ring to the array (with an optimistic border cut, rejecting the events with the true core location in this newly added ring), 88 new detectors, and more than $4000\mathrm{m}^2$ increase in the area of the array.

If we need higher precision for the reconstructed core location in perimeter area of the array, we can use a smaller limit value for the r_p. However, we should decide that if we need higher precision or more sensitive area.

6 Conclusions

In this paper, an existing technique for the rejection of OEASs was optimized. This technique only relies on the data of array detectors and do not need any other supplemental data such as Cherenkov radiation information of EAS. The most usual method for the rejection of an OEAS is border cut, which significantly decreases the sensitive area of the array and overall efficiency of the array. Also, border cut can decrease the extent of cosmic rays' energy, which can be detected by the array.

According to this technique, a parameter called r_p which is the weighted mean distance of triggered detectors from the reconstructed core location is calculated. If r_p for an EAS is more than a certain value, EAS is rejected as an OEAS.

Also, it was shown that, if we used a new method for finding core location called SIMEFIC II, we could significantly increase the sensitive area of the array. In this paper, it was demonstrated that the reconstruction of the core location with better precision could give better results for OEAS identification procedure. So, the procedure of finding OEASs can be optimized using an optimized version of the SIMEFIC II method for finding core location in an array. Another optimization of the OEAS identification procedure was possible if one could find another OSIP with a narrower distribution function and or a severe change of mean function trend on the border of the array.

SIMEFIC II method is not so sensitive to the information of an isolated detector with random large pulse height, because it depends on the information of a pair of detectors and it is very impossible for the two detectors far from core location and near each other to have random high-pulse height simultaneously.

References

[1] HEGRA collaboration, F. Arqueros et al., *Energy spectrum and chemical composition of cosmic rays between 0.3-PeV and 10-PeV determined from the Cherenkov light and charged particle distributions in air showers*, *Astron. Astrophys.* **359** (2000) 682–694, [astro-ph/9908202].

[2] W. Apel, J. Arteaga, A. Badea, K. Bekk, M. Bertaina, J. Blmer et al., *The kascade-grande experiment*, *Nuclear Instruments and Methods in Physics Research Section A: Accelerators, Spectrometers, Detectors and Ass*

[3] H. Hedayati, A. Anvari, M. Bahmanabadi, J. Samimi and M. K. Ghomi, *A new method for finding core locations of extensive air showers*, *The Astrophysical Journal* **727** (2011) 66.

[4] H. Krawczynski, J. Prahl, F. Arqueros, S. Bradbury, J. Cortina, T. Deckers et al., *An optimized method for the reconstruction of the direction of air showers for scintillator arrays*, *Nuclear Instruments and Methods in Physics Research Section A: Accelerators, Spectrometers, Detectors and Associated Equipment* **383** (1996) 431–440.

[5] H. Mayer, *A neural network algorithm for core location analysis at large extended air shower arrays*, *Nuclear Instruments and Methods in Physics Research Section A: Accelerators, Spectrometers, Detectors and Associated Equipment* **317** (1992) 339–345.

[6] D. Heck, G. Schatz, J. Knapp, T. Thouw and J. Capdevielle, *Corsika: A monte carlo code to simulate extensive air showers*, tech. rep., 1998.

[7] A. Ferrari, P. R. Sala, A. Fasso and J. Ranft, *Fluka: A multi-particle transport code (program version 2005)*, tech. rep., 2005.

[8] S. Ostapchenko, *Monte carlo treatment of hadronic interactions in enhanced pomeron scheme: Qgsjet-ii model*, *Physical Review D* **83** (2011) 014018.

[9] H. Hedayati, A. Moradi and M. Emami, *A statistical method for reconstructing the core location of an extensive air shower*, *The Astrophysical Journal* **810** (2015) 68.